Sensors-Experts Associates
1789 Tice Valley Blvd, Walnut Creek, CA 94595, Tel.: 925-354-5599
www.sensors-experts.com

# Modeling Of Permanent Magnets And Ferromagnetic Materials

By Sensors-Experts Associates

Sensors-Experts Associates
1789 Tice Valley Blvd, Walnut Creek, CA 94595, Tel.: 925-354-5599
www.sensors-experts.com

# 1 Background

Modeling of permanent magnets and ferromagnetic materials was carried out with the Comsol Multiphysics finite element analysis (FEA) tool. If the design was axi-symmetrical then modeling was done in 2D axi-symmetrical space, which afforded rapid solutions. In some cases, however, the ramifications of parts misalignment were of main interest. These cases don't posses axial symmetry, and therefore modeling was conducted in 3D space.

Modeling results correspond well to the experimental data, which validates extracted design dependencies.

Permanent magnets for the experimental work were purchased from Emovendo www.emovendo.com. Dimensions and magnetization data were also obtained from this vendor.

Sensors-Experts' customer had to design several magnetic coupling components. Sensors-Experts were tasked with exploring the design space with FEA and other modeling methods, and extracting design dependencies. Some results of this work are presented below.

# 2 Permanent magnet and stainless steel ball

The objective of this study was to analyze an ***Actuator – Force Sensor*** coupling and to maximize developed attractive force.

The actuator shaft was terminated with the cylindrically shaped, axially magnetized NeFeB permanent magnet. The force sensor has a plunger shaped as a 1.75 mm diameter ball. The ball is made of SS316 stainless steel and exhibits weak ferromagnetic properties, $\mu_0 = 100$. The permanent magnet was made of N52 alloy with residual magnetization 1.4 T. The geometry is shown in Figure 1.

The permanent magnet and the plunger ball are supposed to be in intimate contact during actuator operation, which involves vibration along the Z-axis. In simulation, the gap between the ball and the permanent magnet was set to 1 μ to account for possible film and dirt formation on the surfaces. For ease of visualization, the gap shown in Figure 1 is much larger.

Design variables were the diameter and the length of the permanent magnet cylinder. Because the objective was to maximize the coupling force, and the device was to function at benign conditions, the magnet was presumed to be of N52 type, which is the strongest type offered by the vendor.

Modeling was done in 2D axi-symmetrical space. Magnets with diameters of 1/16, 1/8, 3/16, 1/4 inch were considered. The length of the magnet ranged from 1/16 to 1 inch. The results of the simulation are shown in Figure 2 - Figure 3.

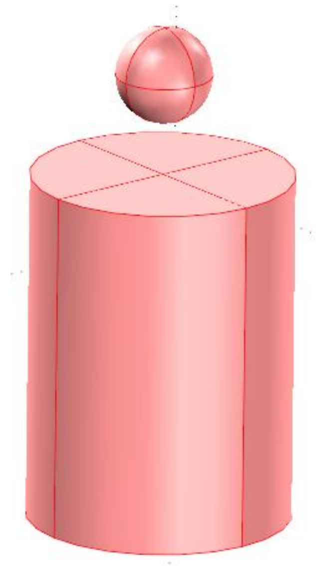

**Figure 1. Cylindrical permanent magnet – SS316 ball geometry. The gap between cylindrical magnet and stainless steel ball was increased 100x for ease of visualization**

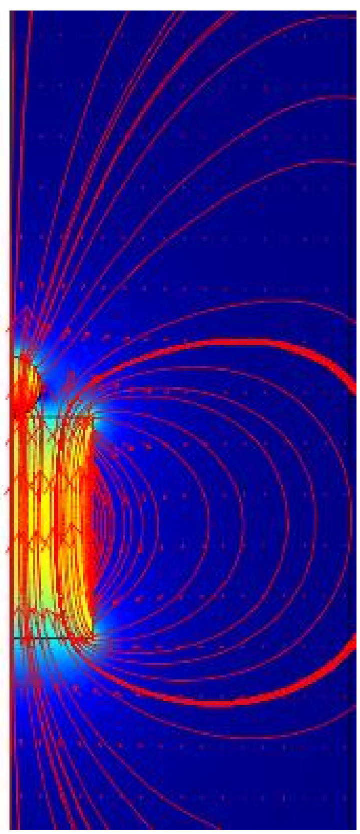

**Figure 2. Results of modeling of cylindrical permanent magnet – SS316 ball geometry. Gap between the magnet and the ball is 1 µ. Color and arrow size represent magnetic field flux density, $\boldsymbol{B}$.**

Extracted design dependencies are shown in Figure 3. As expected, the attractive force increases with the length of the permanent magnet cylinder. However, for each magnet diameter there is a knee on the ***F(L)*** curve beyond which there is a very little force increase. This behavior would be difficult to predict with analytical modeling. On the other hand, with FEA it is quite straight forward.

Another result that was somewhat surprising was the extracted ***F(diam)*** behavior. It turned out that the 1/8 inch diameter magnet delivered the greatest force of all modeled diameters.

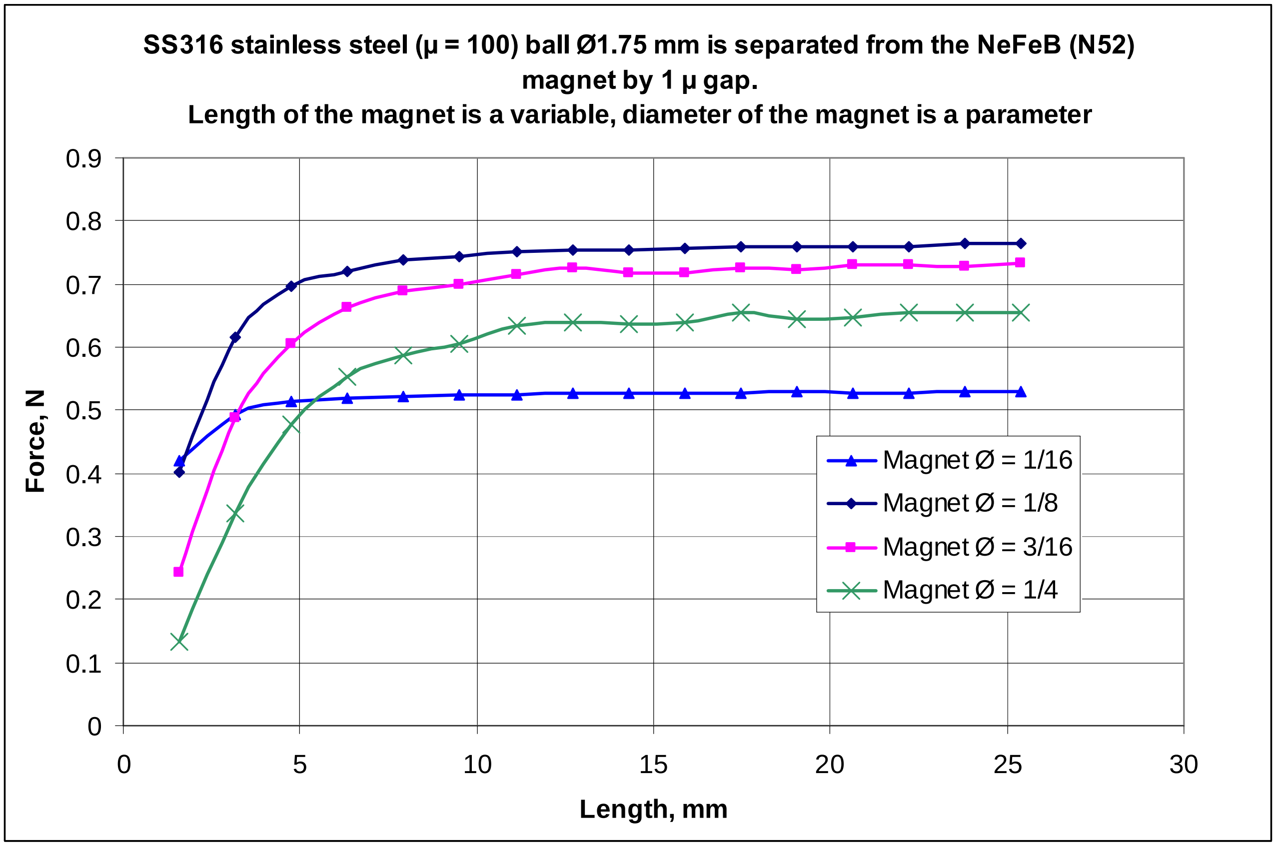


**Figure 3. Design dependencies in a cylindrical permanent magnet – SS316 ball geometry.**

## 3 Progressive force limiter

The objective of this effort was to analyze the design space of the progressive force limiter. The limiter is a device that limits motion of the linear motor. The magnetic limiter consists of two axially magnetized permanent magnet disks facing each other so that magnetization is in opposite directions (Figure 4). One magnet, a movable one, is mounted on the shaft of the linear motor and the other magnet is a stationary one. The repulsive force developed between the pair is expected to be highly non-linear, and increase progressively as the magnets are driven towards each other. The magnetic limiter is a nice alternative to the compression spring, in which the force varies linearly and comes to a hard stop, thereby limiting the motion too abruptly

One of the design objectives was to optimize the preload force, which is exerted when magnets are at the maximum distance away from each other, and to achieve a certain repulsive force at a certain distance when the magnets are close to each other.

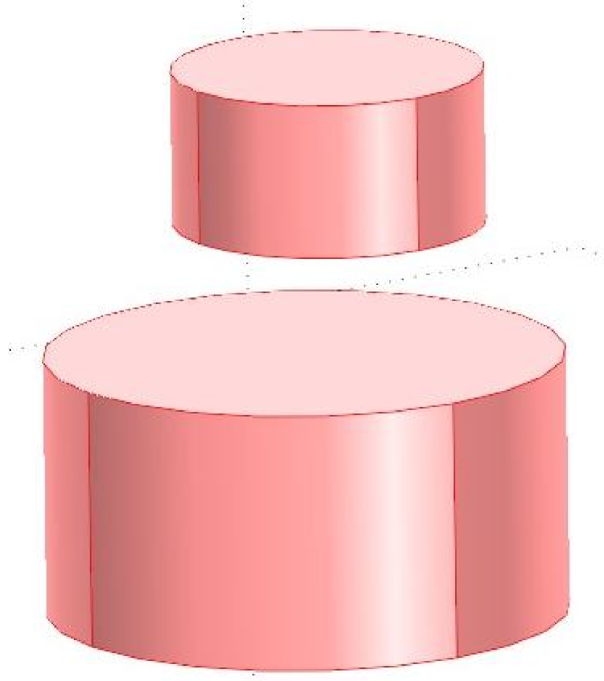

**Figure 4. Ø5/16 x 5/16 magnet is facing Ø3/16 x 3/16 magnet with an intentional axial misalignment of 0.1 mm. Magnets are separated by a 4 mm air gap.**

Another objective was to study the effect of axial misalignment on the repulsive force and on off-axis, i.e. radial force.

The permanent magnets are presumed to be made of N52 alloy with the residual magnetization of1.4 T.

The design variables are the diameter and length of each magnet disk, as well as the axial misalignment between the disks.

## *3.1 Varying diameter of the movable magnet*

During the first set of simulations the geometry was as follows:

- Movable magnet: Ø5/16 x 5/16 inch
- Stationary magnet: Ø - varying x 5/16 inch
- Spacing between magnets: 7 mm
- Misalignment: 0 mm

Simulated dependence of the repulsive force upon the diameter of the stationary magnet is shown in Figure 5. Force increased with the diameter as expected, but only up to a point. Taking this dependence and other design considerations into account, the diameter of the stationary magnet was chosen to be ¾ of an inch, i.e. 19.1 mm.

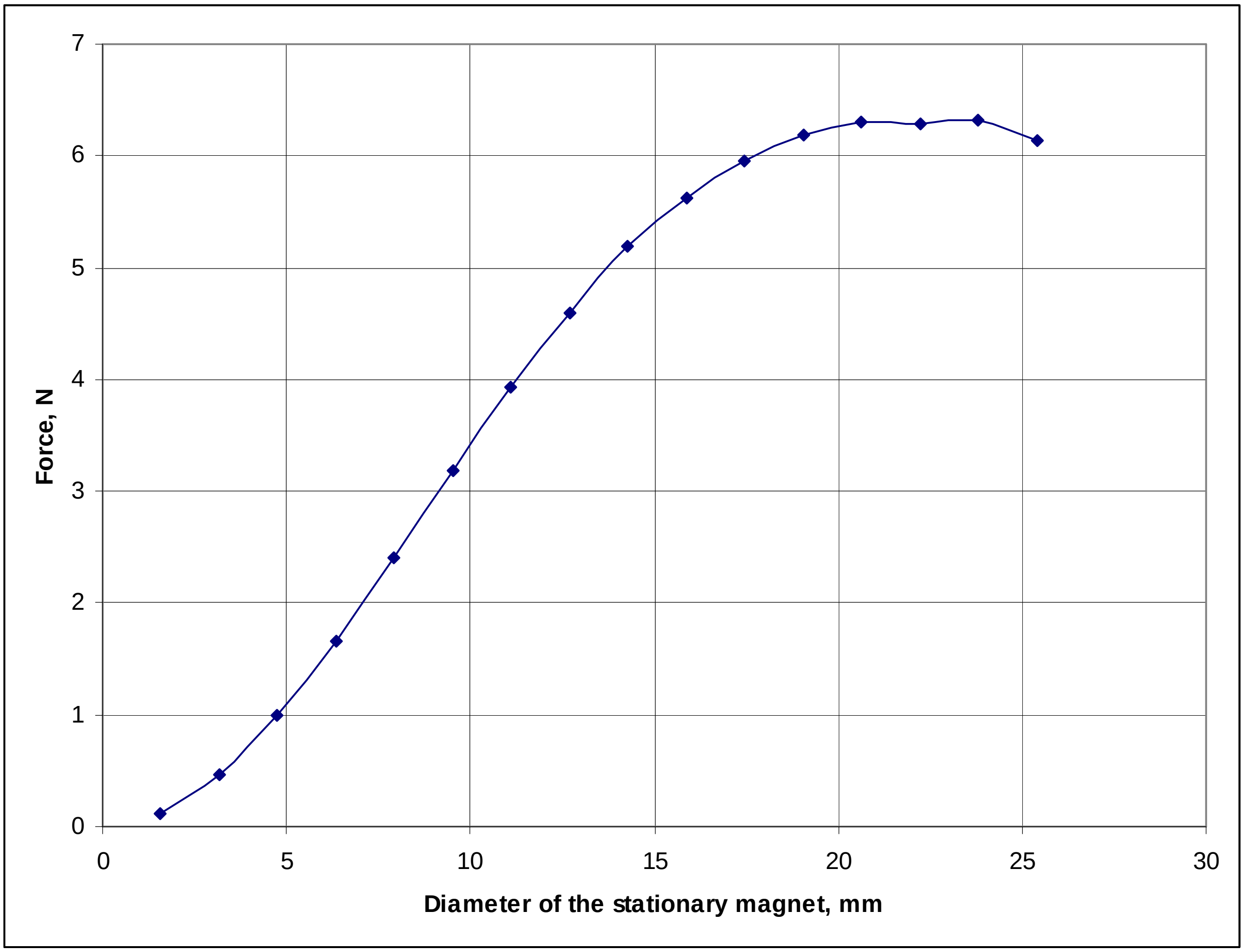


**Figure 5. Simulated dependence of the repulsive force upon the diameter of the stationary magnet**

## *3.2 Varying spacing between the magnets*

With the diameter of the stationary magnet held constant the following study was carried out:

- Movable magnet: Ø5/16 x 5/16 inch
- Stationary magnet: Ø3/4 x 5/16 inch
- Spacing between magnets: varying
- Misalignment: 0 mm

Simulated dependence of the repulsive force upon the spacing between the magnets is shown in Figure 6. As expected, the force increases in non-linear fashion as the magnets are pushed closer. However, at small gaps the repulsive force doesn't rise asymptotically to infinity, as could be anticipated. The reason being that the magnetization of each magnet is not a constant but rather a function of the external magnetic field, generated by another magnet (recall the hysteretic ***B(H)*** curves).

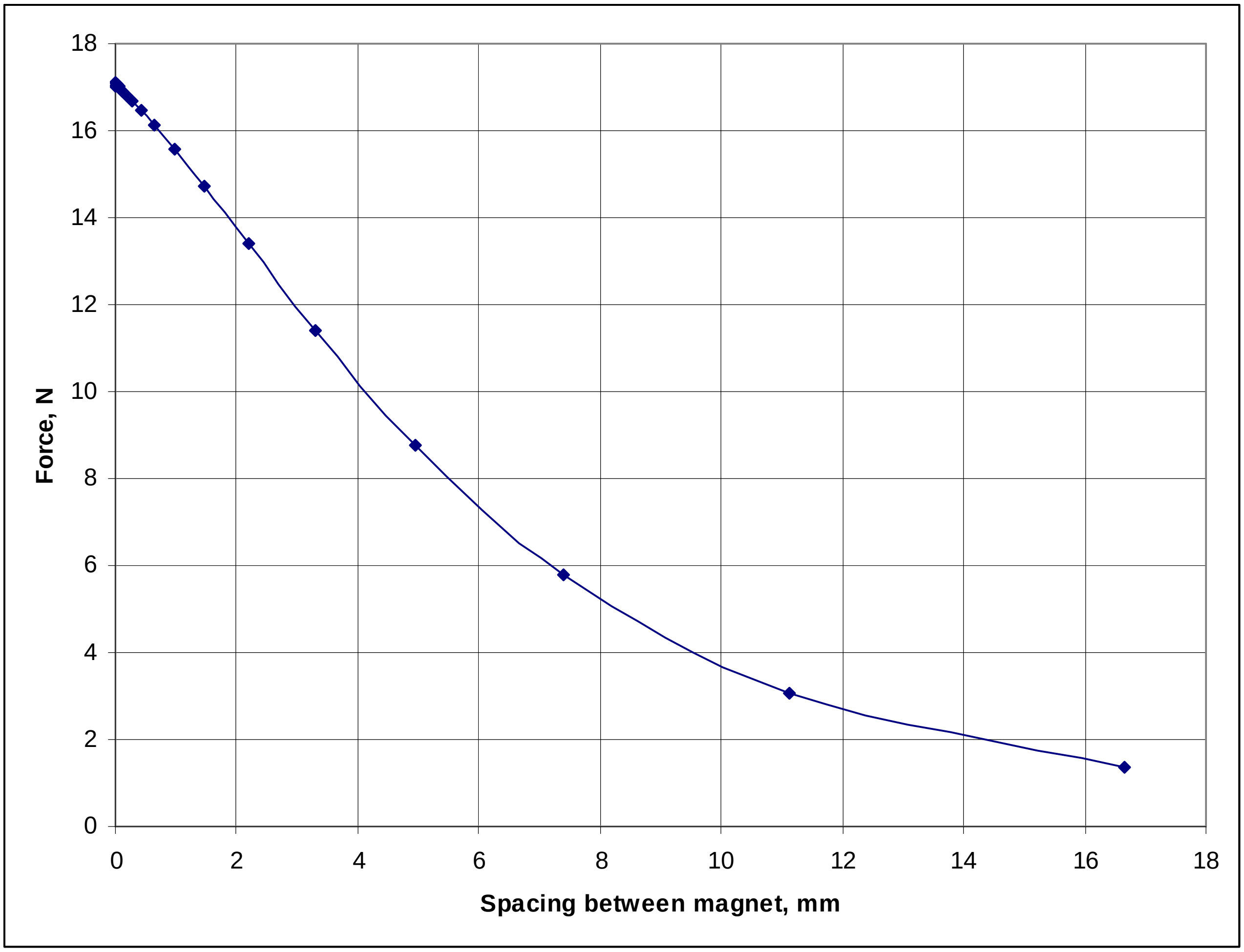


**Figure 6. Simulated dependence of the repulsive force upon the spacing between the magnets**

## *3.3 Varying axial misalignment between the magnets*

During this final set of simulations the geometry was as follows:

- Movable magnet: Ø5/16 x 5/16 inch
- Stationary magnet: Ø3/4 x 5/16 inch
- Spacing between magnets: 7 mm
- Misalignment: varying

Simulated dependence of the repulsive force and the off-axis, i.e. radial, forces upon the axial

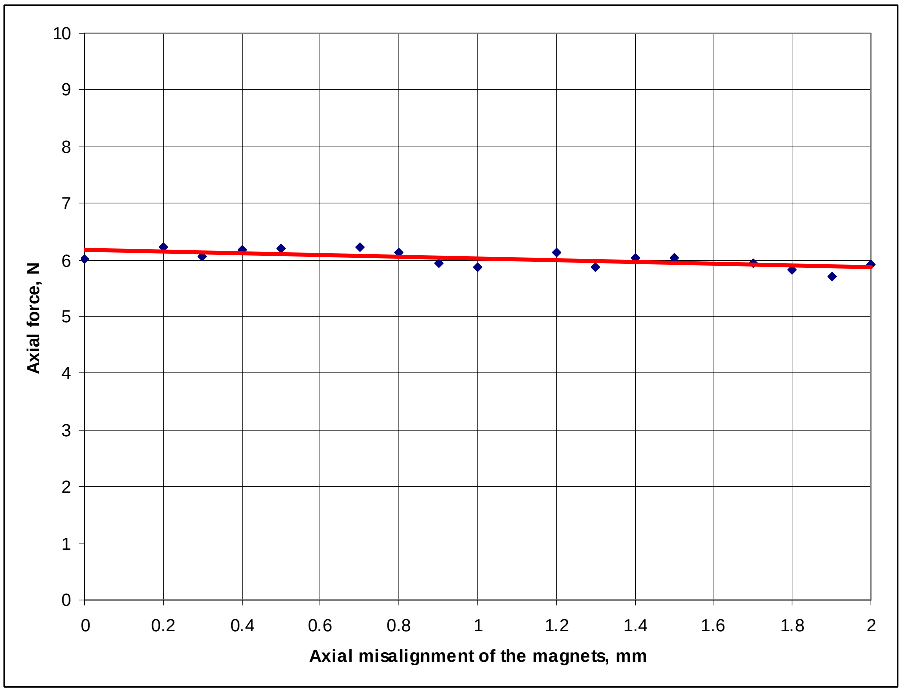


**Figure 7. Simulated dependence of the repulsive axial force upon the misalignment between the magnets**

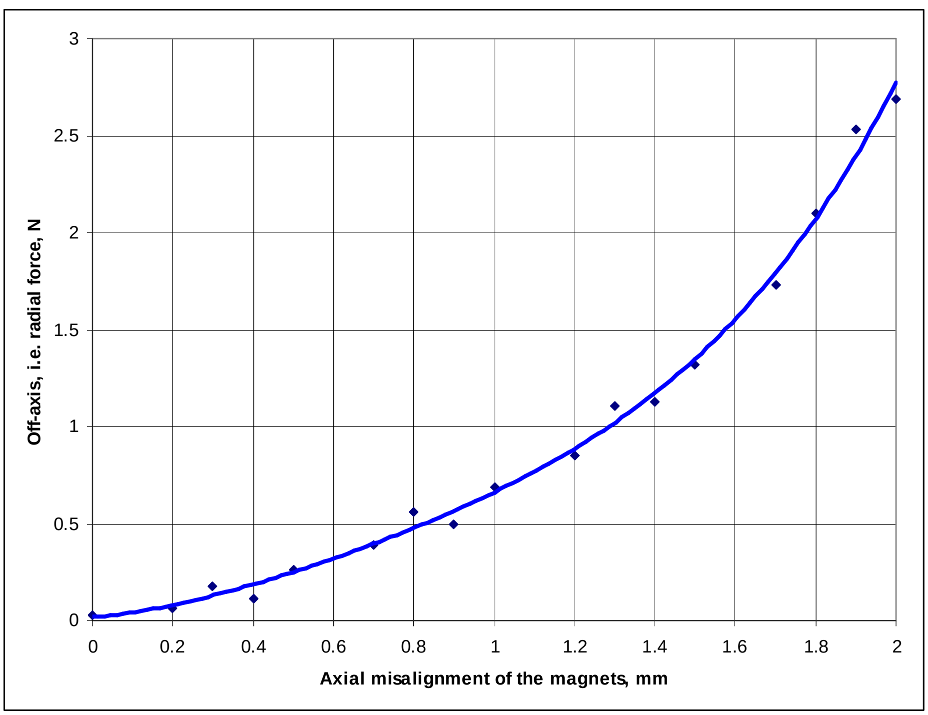


**Figure 8. Simulated dependence of the off-axis, i. e. radial force upon the misalignment between the magnets**

misalignment between the magnets is shown in Figure 7 and Figure 8, respectively. As expected, the axial repulsive force decreases with misalignment.

Misalignment also gives rise to off-axial, i.e. radial force. This is an undesired force that imposes additional requirements on structural components that provide axial stability.

# 4 Conclusions

FEA is a powerful analysis and optimization tool that assists designers working in various physics domains. Sensors-Experts Associates routinely use Comsol Multiphysics and ANSYS Multiphysics FEA packages for various single- and coupled-field modeling applications. In particular, the magneto-static FEA carried out in the course of this project resulted in the extraction of several valuable design dependencies that allow rapid design optimization. It also reduced physical prototyping time and shortened the product development phase.